Heliyon 7 (2021) e05970

Contents lists available at ScienceDirect

Heliyon

journal homepage: www.cell.com/heliyon

Research article

Effect of CO_2 driven ocean acidification on calcification, physiology and ovarian cells of tropical sea urchin *Salmacis virgulata* – A microcosm approach

Muthusamy Anand [a,*], Kannan Rangesh [a], Muthuchamy Maruthupandy [a,b], Govindarajulu Jayanthi [a], Balakrishnan Rajeswari [a], Radhakrishnan Jeeva Priya [a]

[a] Department of Marine and Coastal Studies, School of Energy, Environment and Natural Resources, Madurai Kamaraj University, Madurai, Tamil Nadu 625 021, India
[b] Department of Chemical Engineering, Faculty of Physical Science and Mathematics, University of Chile, Santiago, Chile

ARTICLE INFO

Keywords:
Ocean acidification
Microcosm
Calcification
Biomarkers and ovarian damage

ABSTRACT

In the present study, we depict the structural modification of test minerals, physiological response and ovarian damage in the tropical sea urchin *Salmacis virgulata* using microcosm CO_2 (Carbon dioxide) perturbation experiment. *S. virgulata* were exposed to hypercapnic conditions with four different pH levels using CO_2 gas bubbling method that reflects ambient level (pH 8.2) and elevated pCO_2 scenarios (pH 8.0, 7.8 and 7.6). The variations in physical strength and mechanical properties of *S. virgulata* test were evaluated by thermogravimetric analysis, Fourier transform infrared spectroscopy, X-ray diffraction analysis and scanned electron microscopy analysis. Biomarker enzymes such as glutathione-S-transferase, catalase, acetylcholine esterase, lipid peroxidase and reduced glutathione showed physiological stress and highly significant ($p < 0.01$) towards pH 7.6 and 7.8 treatments. Ovarian cells were highly damaged at pH 7.6 and 7.8 treatments. This study proved that the pH level 7.6 and 7.8 drastically affect calcification, physiological response and ovarian cells in *S. virgulata*.

1. Introduction

"Ocean acidification"- refers to reducing the ocean pH from any starting point to any end point in the pH scale due to high level atmospheric CO_2 mixing with seawater and subsequent change in the seawater carbonate system (IPCC, 2011). In pre-industrialisation time, the level of atmospheric CO_2 was 280 ppm whereas the current level of atmospheric CO_2 is >400 ppm; this has resulted in a reduction of ocean pH from 8.25 to 8.14 (Orr et al., 2005; Iglesias-Rodriguez et al., 2010). If the "business as usual scenario" continues, the excess CO_2 emission will reduce pH up to 0.5 units by the end of this century (Hall-Spencer et al., 2008).

Marine calcifiers are sensitive to ocean acidification and are affected by two possible routes of action (Yang et al., 2016). One is the seawater acidity makes corrosion or deformation of the animal shell due to prolonged exposure and another one is by the demand of carbonate ions in seawater which is the essential source for shell formation. The latter is due to hydrogen ions dissociation and its incorporation with existing carbonate ions followed by transformation into bicarbonate ions. As a result, abundant level of bicarbonate is deposited in seawater. Here, shelled animals can only imbibe carbonate ions from seawater to build its outer skeleton shell; the process called calcification or biomineralization and cannot uptake bicarbonate forms instead of carbonate. Thus, increasing level of CO_2 lowers the calcium carbonate saturation level hence it is less favourable to the precipitation of calcium carbonate shells and more favourable for the dissolution of skeletons (Zeebe, 2012). Reduction of calcification rate has been observed in variety of taxonomic groups especially in corals and molluscs (Michaelidis et al., 2005; Kuffner et al., 2008). Calcification rate in shelled organisms is varied by the level of $CaCO_3$ saturation states hence the construction of $CaCO_3$ is to be proportional to their saturation level (Ilyina et al., 2009). In addition, the external acid-base influence of seawater causes the animals to alter the regular metabolism, mainly because of ionic fluctuations.

Ocean acidification has a profound impact on the size and weight of shells and skeletons of marine calcifiers (Spicer et al., 2007; Watson et al., 2012; Duquette et al., 2017; Qu et al., 2017; Coll-Llado 2018). Sea urchins are marine calcifiers which play an important ecological role as major grazers in the marine ecosystem, as well as being an experimental model organism for developmental biologists. They directly absorb most of the essential nutrients they require from the seawater in which they live (Vidavsky et al., 2014), hence it is believed that these organisms are

* Corresponding author.
E-mail address: anandm21@yahoo.com (M. Anand).

https://doi.org/10.1016/j.heliyon.2021.e05970
Received 10 November 2020; Received in revised form 6 January 2021; Accepted 8 January 2021

the first responders to any chemical imbalance in the acidified waters. Sea urchin larvae exposed to low pH has negatively influenced the digestive efficiency of the organisms (Stumpp et al., 2012). High CO_2 induced ocean acidification affect the sea urchin's fertilization, larval growth and physiology, juvenile and adult growth and reproduction (Emerson et al., 2017; Brothers et al., 2015; Bray et al., 2014; Ross et al., 2011). Sewell et al. (2014) reported that the fertilization success of sea urchin would significantly get affected as consequence of ocean acidification phenomenon for the next fifty years. In such case, ocean acidification phenomenon could lead to cascading effects in the complex marine food web.

Sea urchin *Salmacis virgulata* belong to the phylum Echinodermata is the most common species distributed in the near shore marine ecosystem of the Gulf of Mannar waters, South East Coast of India where they play an important ecological role in shallow subtidal region as grazers of marine algae. The Gulf of Mannar is a large shallow bay forming part of the Laccadive Sea in the Indian Ocean. The Gulf is noted for religious tourism (Kathiravan et al., 2017), trawl net operations (AmalaShajeeva et al., 2017) and Tuticorin sea port traffic posing a major threat of anthropogenic CO_2 emission and ocean acidification. The mean annual rainfall of the region ranged from 762 mm to 1270 mm (Neelakantan, 1998) and pH from 7.0 to 8.3 (Anandakumar and Thajuddin 2013) respectively. pH of Gulf of Mannar waters remain alkaline between 7.7 and 8.5 (Arumugam et al., 2013; Sivakumar, 2009) due to various factors like photosynthesis, respiration, decomposition and freshwater inflow (Rajasegar, 2003). In this scenario of high spatiotemporal variation of pH and the "business as usual" condition of anthropogenic source of CO_2 input, there is no concrete data on the impact of ocean acidification on calcifiers of the Gulf of Mannar region.

The present study tests the hypothesis that the reduced ocean pH and $CaCO_3$ availability will adversely affect the biomineralization process of shell formation by direct physiological stress. Ocean acidification can induce oxidative stress due to change in the acid-base regulation and formation of reactive oxygen species. Hence, the increasing anthropogenic CO_2 emission and OA is a testament to weaken the physiology of sea urchin. The profound impact of ocean acidification in the sea urchin, *S. virgulata* was studied by choosing four different pH levels that depict the ambient 8.2 in Gulf of Mannar waters (Arumugam et al., 2013) and elevated pCO_2 levels using CO_2 gas bubbling method (Riebsell et al., 2010) in microcosm setup that represent future ocean acidification conditions such as pH 8.0, 7.8 and 7.6 (Clark et al., 2009; Martin et al., 2011). Here, the term microcosm refers to the setup of miniature environment in terms of glass bowls or part of ex situ environment for studying the effects on selected number of samples. So far, large number of studies have started to focus on the role of elevated pCO_2 condition on biomineralization properties of marine calcifiers; however, the role of physiology especially biomarkers have been poorly studied hence we assessed the biomarker enzyme responses as well as the ovarian cell condition to ambient pH and reduced pH conditions.

2. Materials and methods

2.1. Animal collection and acclimatization

Sea urchins (*S. virgulata*) with a test diameter between 7.2 cm and 8.7 cm were collected from Keelakarai coastal waters (9°06′38.2″N 78°50′02.3″E) of the Gulf of Mannar region, Southeast coast of India, in a depth of approximately five meters by SCUBA diving. From the collection site, the animals were transferred to Pudumadam Field Research lab using refrigerated van covering a distance of 35 kms in one and half hours. The animals were transferred into seawater tanks (50 L) with an aerator, and acclimatized for seven days. Here Acclimation refers the animal accustomed to a new climate or to new conditions whereas acclimatization refers to the process in which an individual organism adjusts to a change in its environment, allowing it to maintain performance across a range of environmental conditions. Apart from control, all animals were acclimatized with the respective low pH seawater. Seawater was renewed twice per day. For first three days of acclimation, filtered seawater collected from sea urchin sampling site was used. For another four days of acclimatization, the seawater collected from near shore (approximately 300 m distance) to Marine field research lab at Pudumadam coast, Gulf of Mannar region was used for subsequent water renewal. Animals were fed with seaweeds (*Sargassum* spp) during acclimatization.

2.2. Experimental setup

CO_2 perturbated microcosm setup demonstrated by Riebsell et al. (2010) was modified and adapted for the laboratory experiment (Figure 1). Four different pH levels were selected based on the prediction represented by Gattuso and Lavigne (2009) and Wolf-Gladrow et al. (2007) using R software - Searcarb package that reflect an ambient level (pH 8.2) and three elevated pCO_2 scenario levels of ocean acidification (pH 8.0, 7.8 and 7.6). For CO_2 gas bubbling, the CO_2 gas cylinder was connected to three reservoir tank containing filtered seawater each 10 L prepared from sand filtration then the CO_2 was released slowly to the extent to reach the desired seawater pH (7.6, 7.8, and 8.0). CO_2 perturbation was not carried out in fourth reservoir tank which was the control (pH 8.2). Continuously, from these reservoir tanks, CO_2 perturbed seawater and ambient seawater was opened to four open cell glass bowls (each 7 L) and the same setup was duplicated. Three acclimatized healthy sea urchins (average test diameter size of 8.5 cm) were introduced into each experimental glass bowls and replicative glass bowls with CO_2 treatments. Feeding was stopped on last day morning of acclimatization. After 24 h, the experiment was started. Regular pH monitoring using pH meter (accuracy $\pm$0.001 pH) was done in each experimental chamber every 4 h in day and night. During slight deviation in pH, CO_2 perturbed seawater was opened from reservoir tank to recompense for maintaining the desired pH. Seawater was siphoned and renewed twice per day. The experiment was run for 14 days.

2.3. Physicochemical parameters

For every 4 h, the pH, temperature, salinity, and total alkalinity of seawater were measured during the experiment. Among these, pH and temperature both was observed using pH ion meter (Eutech bench pH/Ion meter Model pH 2100). Salinity was checked using hand refractometer (Atago Master-S). Total alkalinity was measured by volumetric method using phenolphthalein and bromocresol green indicators and H_2SO_4 as acid titrant after poisoning with mercuric chloride (APHA, 2005). Among the observed parameters, pH, temperature, salinity and total alkalinity were given as input for CO2calc software (Version 1.0.3.) and the other associated seawater carbonate parameters such as Ω_{Ca}, Ω_{Ar}, HCO_3, CO_3, pCO_2, and TCO_2 were calculated. Two ml of hemolymph was extracted using syringe needle on the animal's oral side and measured its pH on alternate days (once in 48 h) using the pH ion meter. Experiment was done at fourteenth day. Three sea urchins were randomly selected from each treatment and their shells, spines, digestive tissues and ovary were dissected out and processed for further analysis.

2.4. Biomineralization assays

The following assays were carried out to qualitatively analyze the calcium carbonate in *S. virgulata* test contents to study the negative changes in response to different pH treatments. Shell powder samples of *S. virgulata* were prepared by sunlight drying for 48 h then crushing and grinding of whole test using REMI laboratory blender. Fourier Transform Infrared Spectroscopy (FTIR) analysis was carried out to get an infrared spectrum of *S. virgulata* shell powder (control) at the wave number range between 400 and 4000 cm^{-1} with the 2 cm resolution of wave number detection using FTIR 8400S Shimadzu with Germanium coated KBr Plate. Thermogravimetric Analysis (TGA) was carried out to analyse mass

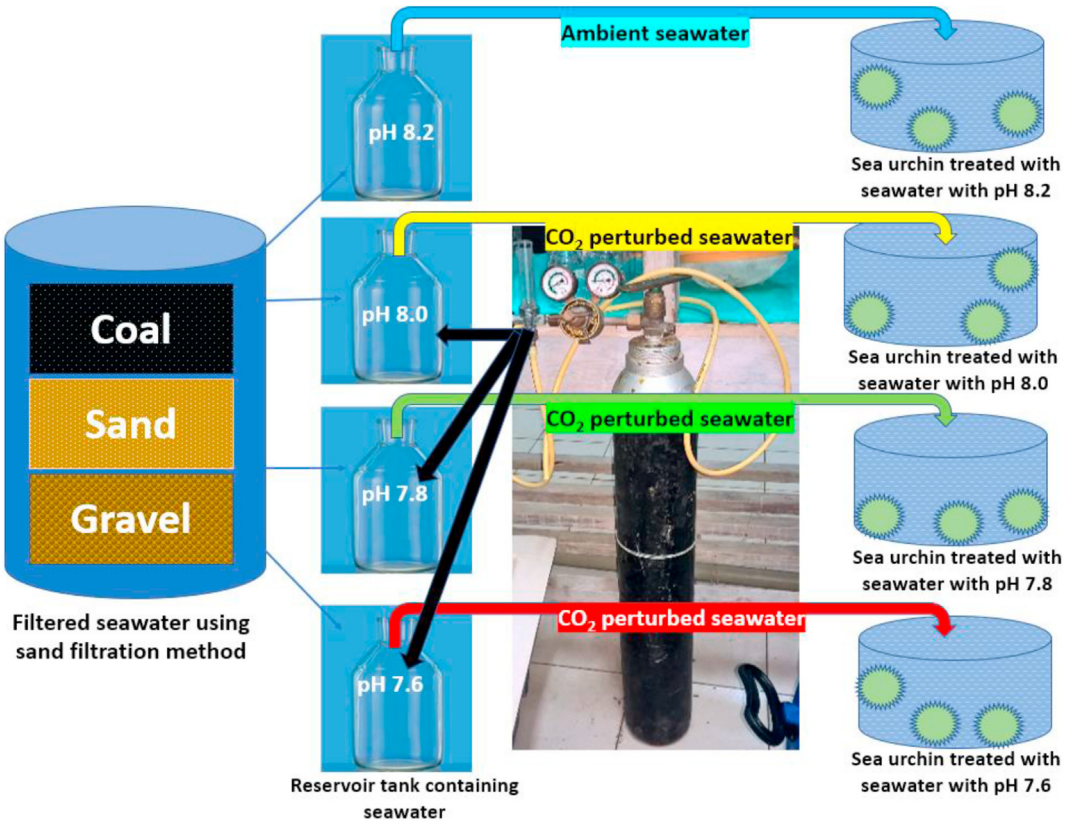

Figure 1. Laboratory set up of CO_2 perturbated microcosm experiment.

properties of the sea urchin shell powder for all pH treatments at a temperature range between 21 °C and 990 °C (Exstar 6000). X-Ray Diffraction Analysis (XRD) was carried out to determine the phase crystalline nature of the sea urchin shell powder with different pH conditions at the copper 2θ range of 10°–80° in a fixed time mode at room temperature (X'Pert Pro). Basal spines of sea urchin were examined under Scanned Electron Microscopy (SEM) analysis (Model: TESCAN VEGA3 SBH) operated at 5 kV and its number per area calculation were analyzed using ImageJ software.

2.5. Biomarker assays

Biomarkers have the important role in indication of physiological stress to the pH treated animals. After completion of 14th day experiment, *S. virgulata* gut tissues from different pH treatments were immediately ground with phosphate buffer solutions and these were centrifuged to obtain enzyme sources. These enzymes were used for biomarker assays namely Glutathione-S-Transferase (GST), Catalase (CAT), Acetylcholine Esterase (AChE), Lipid Peroxidase (LPx) and Reduced Glutathione (GSH) assays using centrifugation followed by spectrophotometer. Two samples from each treatment were assayed. These enzymes indicate the physiology related response against the oxidative stress due to changes in acid base regulation. AChE activity was measured using the substrate analogue namely acetylthiocholine iodide which converted to thiocholine. Chemical reaction of thiocholine with dithionitrobenzoic acid (DTNB) - the chromogenic substrate makes the formation of nitrobenzoic acid - yellow anion that absorbs at 412 nm (Ellman et al., 1961). CAT activity was determined using Sinha (1972) method by observing decrease of H_2O_2 in absorbance at 570 nm and enzyme activity was expressed as H_2O_2 consumed/min/mg protein. GST activity was tested by spectrophotometer at 340nm by enumeration of CDNB (1-chloro-2, 4-dinitro-benzene) conjugated with reduced glutathione as a function of duration (Habig et al., 1974). LPx level was assayed by quantification of malondialdehyde (MDA), a decomposed product of PUFA (polyunsaturated fatty acids) and hydro peroxides were determined using thiobarbituric acid reaction method described by Ohkawa et al. (1979). MDA's absorbance was read at 532 nm following the removal of fluctuated materials using centrifugation and it was expressed in nano moles malondialdehyde (MDA)/mg protein. GSH level was quantified according to Moron et al. (1979) method by measuring the reaction with 5, 5'dithiobis (2 nitro benzoic acid) DTNB to give the absorbance at 412 nm and the level was measured as μM of GSH mg^{-1} protein.

2.6. Histology sectioning

Female gonad tissues of *S. virgulata* (three numbers) from each treatment were dissected out for histology sectioning. Automated tissue processor was used for this test (Lang et al., 2006). The gonads were fixed in Bouin's solution (a histological fixative – prepared using 15:5:1 ratio of saturated picric acid in 95% ethanol: formaldehyde: glacial acetic acid) for 24 h. Later, the gonads were processed by dehydration, cleared in xylene and finally embedded in paraffin wax. The block has been sectioned at 5 μm using a rotary microtome followed by deparaffination and washing. The samples were stained using haematoxylin and eosin. Five sections were selected and one and the one which looked clear tissue damage was used. Finally, the prepared slides were examined under the light microscope which can able to detect colour i.e., RGB images at resolution of 40X magnification.

2.7. Data analysis

The results of FTIR, XRD and TGA graphs were plotted with origin pro-8.1. Descriptive statistics was used for physicochemical parameters and One-way ANOVA was used for biomarker enzyme responses using Microsoft Excel 2007.

3. Results

3.1. Physicochemical parameters

The mean pH, temperature, salinity, total alkalinity in four different pH treated seawaters and the respective carbonate parameters such as Ω_{Ca}, Ω_{Ar}, HCO_3, CO_3, pCO_2, and TCO_2 were given in Table 1. These results represent the mean SD (N = 80 data collected for 14 days × 6 times per day) of microcosm experiment observation. There were no mortalities observed during the experiment. The real time extraction and observation of sea urchin haemolymph pH was 7.24 ± 0.08, 7.68 ± 0.05, 7.66 ± 0.07 and 7.94 ± 0.04 (mean with standard deviation) during all pH treatments.

3.2. Biomineralization

3.2.1. FTIR

The representative FTIR spectral analysis from chosen replicates studied with the wide range from 400 to 4000 cm^{-1} of the *S. virgulata* shell powder exposed in three experimental pH and control showed distinct peak values (Figure 2). The peak at 713cm^{-1} represents the double degenerate planar bending (V4) in calcite phase of $CaCO_3$ in *S. virgulata* exposed to all four pH treatments. This is due to asymmetric bending mode of carbonate ions. The out of plane bending (V2) was displayed by a peak at 875 cm^{-1} in *S. virgulata* shell powder exposed to pH 8.2 (control) and pH 8.0 treatments whereas a similar V2 peak at 873 cm-1 was found in pH 7.8 and 7.6. These characteristics could be derived from the symmetric bending mode of carbonate ions. The peak at 1417 cm^{-1} showed the doubly degenerate planar bending (V3) in calcite structure for $CaCO_3$ in *S. virgulata* shell powder exposed to pH 8.2 (control) and pH 8.0 treatments whereas a similar V3 peak at 1415 and 1411 cm^{-1} was found in pH 7.8 and 7.6 respectively. It represents the presence of aromatic groups C=C in fingerprint region. The peak 2521 cm^{-1} indicated the N–H bonds represent ammonium ions. The peak range between 2926 and 2928 cm^{-1} signs the change in methylene group with compare to control. The structure of bonds elucidated for the peaks between 3414cm^{-1} from pH 7.6 and 3421 cm^{-1} from pH 8.2 enunciated the change in O–H stretching mode in *S. virgulata* test skeleton.

3.2.2. TGA

Thermal analysis of *S. virgulata* shell powder revealed a rapid calcium carbonate weight loss in pH 7.6 and 7.8 compared to the pH 8.0 and 8.2 (Figure 3). The initial weight loss occurred when the temperature was below 100 °C which denotes removal of moisture content. Further increase in temperature revealed subsequent weight loss of subsequent organic molecules. The weight loss of amorphous calcium carbonate in the test shell powder was significant between high and low CO_2 conditions. A narrow range of temperature difference was observed for I, II, III and IV weight loss for pH 7.6 at 235 °C, 250 °C, 598 °C and 601 °C and for pH 7.8 at 272 °C, 286 °C, 609 °C and 616 °C respectively. Similarly, for pH 8.0 I, II, III and IV weight loss were recorded at 417 °C, 435 °C, 668 °C and 674 °C whereas for pH 8.2 at 477 °C, 495 °C, 686 °C and 698 °C.

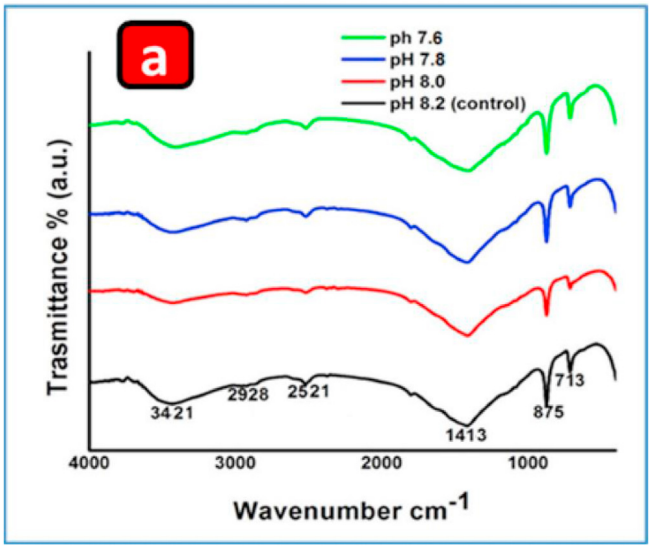

Figure 2. FTIR spectra of control (8.2) and different pH (8.0, 7.8 and 7.6) treated sea urchin shell powders.

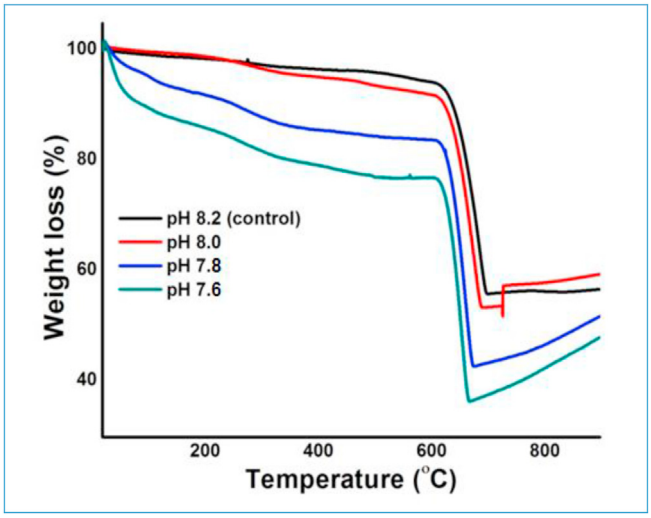

Figure 3. Weight loss thermogram pattern of control (8.2) and different pH (8.0, 7.8 and 7.6) treated *S. virgulata* shell powders. Each sample showed gradual weight loss based on the pH treatment.

Table 1. Physicochemical parameters of seawater during the experiment.

Parameters	pH 7.6	pH 7.8	pH 8	Control (pH 8.2)
pH	7.63 ± 0.02	7.81 ± 0.03	8.00 ± 0.01	8.26 ± 0.04
Temp (°C)	28.5 ± 0.54	28.46 ± 0.54	28.49 ± 0.55	28. 54 ± 0.54
Sal	30.69 ± 1.18	30.32 ± 1.18	30.23 ± 1.11	30.28 ± 0.95
TA (μmol kg^{-1})	1942 ± 43	1978 ± 23	2066 ± 11	2148 ± 7.2
pCO_2 (μatm)	2228.35 ± 92.99	692.20 ± 70.25	197.90 ± 11.00	89.45 ± 18.33
TCO_2 (μmol kg^{-1})	1010.53 ± 22.52	929.48 ± 3.30	869.70 ± 8.57	765.70 ± 32.11
HCO_3 (μmol kg^{-1})	940.06 ± 25.00	879.13 ± 0.46	777.78 ± 14.82	634.29 ± 46.38
CO_3 (μmol kg^{-1})	11.47 ± 1.89	31.88 ± 5.19	86.64 ± 6.68	129.029 ± 14.81
Ω_{Ca}	0.28 ± 0.04	0.80 ± 012	2.18 ± 0.14	3.25 ± 0.34
Ω_{Ar}	0.19 ± 0.03	0.52 ± 0.08	1.43 ± 0.10	2.14 ± 0.24

3.2.3. XRD

The XRD patterns of powdered *S. virgulata* shell under different pH exposures such as 7.6, 7.8, 8 and 8.2 (control) represented the structural properties of biomineral phases at 2θ values from 10° to 80° (Figure 4). In all pH treatments, the 2θ position showed peak 29.8° which is also known as the position of reflection d (104) which confirms the structure of calcite in all samples. The other peak positions also represented the calcite peak such as 23.3° d (012), 31.7° (006), 36.2° (110), 39.8° (113), 43.5° (202), 47.8° (018), 48.5° (116), 58.3° (122), 65.7° (300) and 78.3° (1112) but less intense than peak 29.8° (104) across the shell samples exposed to all pH treatments. The given XRD patterns were assigned for calcite and amorphous calcium carbonate (ACC). The calcite crystals were available for 2θ value at 23.1, 29.6°, 36.2°, and 39.8° and the ACC crystal were available at 28.0°, 31.7°, 46.4°, 57.0 and 71.1°. Compared to pH treated shell powders the control was predominantly composed of calcite type of calcium carbonate. In low pH exposed shells the reduced calcite peak was seen whereas in control (8.2) the peak distinctly showed the calcite blooming which denotes the predominance of calcium carbonate content.

3.3. SEM imaging

The SEM imaging of the basal spine region of *S. virgulata* exposed to all pH treatments were given in Figure 5 a-e. The basal spine surface found corroded with cracks and breaks in pH 7.6 treatments whereas no crack found in pH 8.2 and 8.0. The basal spine surface has different numbers of pores in each pH treatments and number per area has been calculated. Large number of pores found in pH 7.6 was $29 \times 10^{-2}/\mu m^2$ whereas $19 \times 10^{-2}/\mu m^2$ found in pH 7.8. Average number of pores found in pH 8.0 was $17 \times 10^{-2}/\mu m^2$ whereas $13 \times 10^{-2}/\mu m^2$ found in pH 8.2. These attributed that the calcite in *S. virgulata* spines exposed to low pH treatments lead to demineralization, dissolution and corrosion.

3.4. Biomarker assay

The enzymatic response of *S. virgulata* in control and pH treated conditions varied highly significant ($p < 0.01$) and their varying patterns ascertained that the animals were being stressed. The ANOVA for each enzymatic response were given in Table 2. AChE and CAT (Figure 6 a and b) levels were significantly decreased in pH 8, 7.8 and 7.6 when compared with control. GST, LPx and reduced glutathione (Figure 6 c, d and e) levels were significantly increased in pH 8, 7.8 and 7.6 when compared to pH 8.2. AChE activity in hypercapnia condition with maximum decrease was observed at 0.043 μM ACTI/min^{-1}/mg^{-1} protein at pH 7.6 compare to remaining pH treatments. The CAT activity also reduced at 0.032 mM H_2O_2 consumed/min^{-1}/mg^{-1} protein in pH 7.6 whereas maximum activity observed at 0.061 mM H_2O_2 consumed/min^{-1}/mg^{-1} protein in pH 8.2. GST had maximum activity at 0.078 μM GSH & CDNB conjugate formed min^{-1}/mg^{-1} protein in pH 7.6 and minimum activity at 0.052μM GSH & CDNB conjugate formed min^{-1}/mg^{-1} in pH 8.2. In addition, GSH showed higher response at 0.321 and lower response at 0.125 μM of GSH/min^{-1}/mg^{-1} protein for pH 7.6 and 8.2 respectively. LPx showed higher response at 0.903 and lower response at 0.125 nM MDA formed/$min^{-1/}mg^{-1}$ proteins for pH 7.8 and 8.2 respectively. The R^2 value of AchE, CAT, GST, LPx and GSH were 0.416, 0.2652, 0.0061, 0.1044 and 0.4521 respectively. The regression/trend line of AchE, CAT, GST, LPx and GSH were polynomial, power, polynomial, exponential and logarithmic respectively.

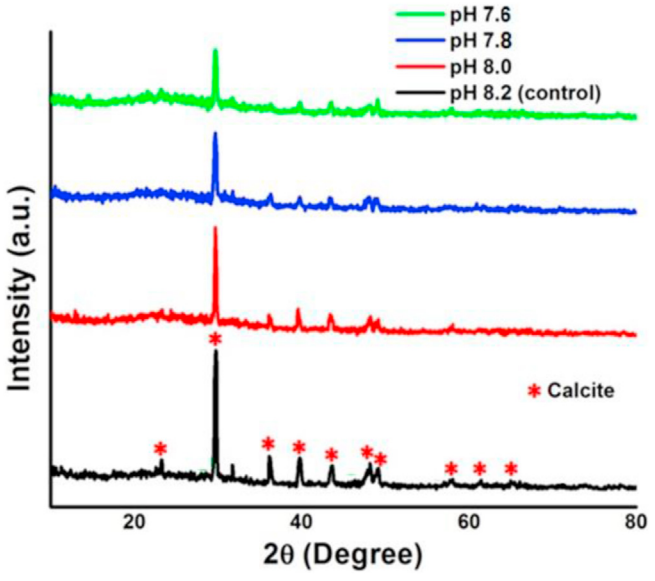

Figure 4. X-ray diffractograms of different pH (8.0,7.8 and 7.6) treated and control (8.2) *S. virgulata* shell powders. Calcite peak is shown with distinct symbols and the longest peak in pH 8.2 indicated the calcite blooming.

3.5. Histopathology

The gonad sections of *S. virgulata* exposed to different pH exposures consist of ovaries with mature oocytes. The control animal possessed mature ovaries with vitellogenic oocytes and the treated animal of pH 8.0, 7.8, 7.6 showed lesions in oocytes (Figure 7 a-d). In addition, the animals from the pH 8.0 showed slight disruption in the density of egg cell whereas the pH of 7.8 and pH 7.6 showed the destruction of cell envelope and more disruption in the density of egg cell and globules of accessory cells intruding an oocyte. Particularly these cell envelopes are jelly coat of ovaries, which has polysaccharides with unique structures. These polysaccharides are very crucial for stimulating the acrosome reaction in species-specific manner. This event is commonly occurred during pre-fertilization stages in terms of binding of sperm and fusion with the egg. Cell disruption and rupture was visible in gonads exposed to pH 7.6 and pH 7.8. Gonad lesions were not found in ovarian cells exposed to control pH 8.2 whereas slight gonad lesions and damage in egg jelly were found in *S. virgulata* exposed to near future acidification pH 8.0.

4. Discussion

Marine calcifiers produce skeletal structures of carbonate in the form of aragonite and calcites (Kawahata et al., 2019). In Echinoderms, two forms of $CaCO_3$ are available i.e., Mg-Calcite and Amorphous Calcium Carbonate (ACC) (Addadi et al., 2003). Amorphous calcium carbonate has important function in $CaCO_3$ formation process as a response of transient precursor phase of calcite or aragonite. Six different forms of $CaCO_3$ exist in nature namely ACC, calcite, aragonite, vaterite, monohydrocalcite and Ikaite. Interplay of one form of $CaCO_3$ to other form reported in many animals. For instance, nacre shells purely made up of aragonite crystal and they can transform to hydroxyapatite by hydrothermal transformation in high pressure (Agaogullari, 2012). Sea urchins have complex skeletal structure; though inter-relation among amorphous calcium carbonate, calcite and intra-crystalline organics is not clear; the biomineralization process in sea urchin is well documented where the transient form of hydrated ACC dehydrates to form ACC and subsequently transformed to calcite (Wolpert and Gustafson 1961; Brecevic and Nielsen 1989; Clarkson et al., 1992; Beniash et al., 1997; Decker et al., 1987; Yutao Gong et al., 2012). Sea urchin test and spicules consist of calcite and magnesium (Drozdov et al., 2016) that grow from a single calcite crystal seed by transformation of a transient ACC phase (Beniash et al., 1999). The possible influence of intra-crystalline organics in sea urchin on size and orientation of calcite crystals is evident from the studies conducted by Berman et al. (1988; 1990 and 1993) where the extract of the skeletal parts from *Paracentrotus lividus* revealed a conchoidal fractured surface for the calcite crystals grown in the presence

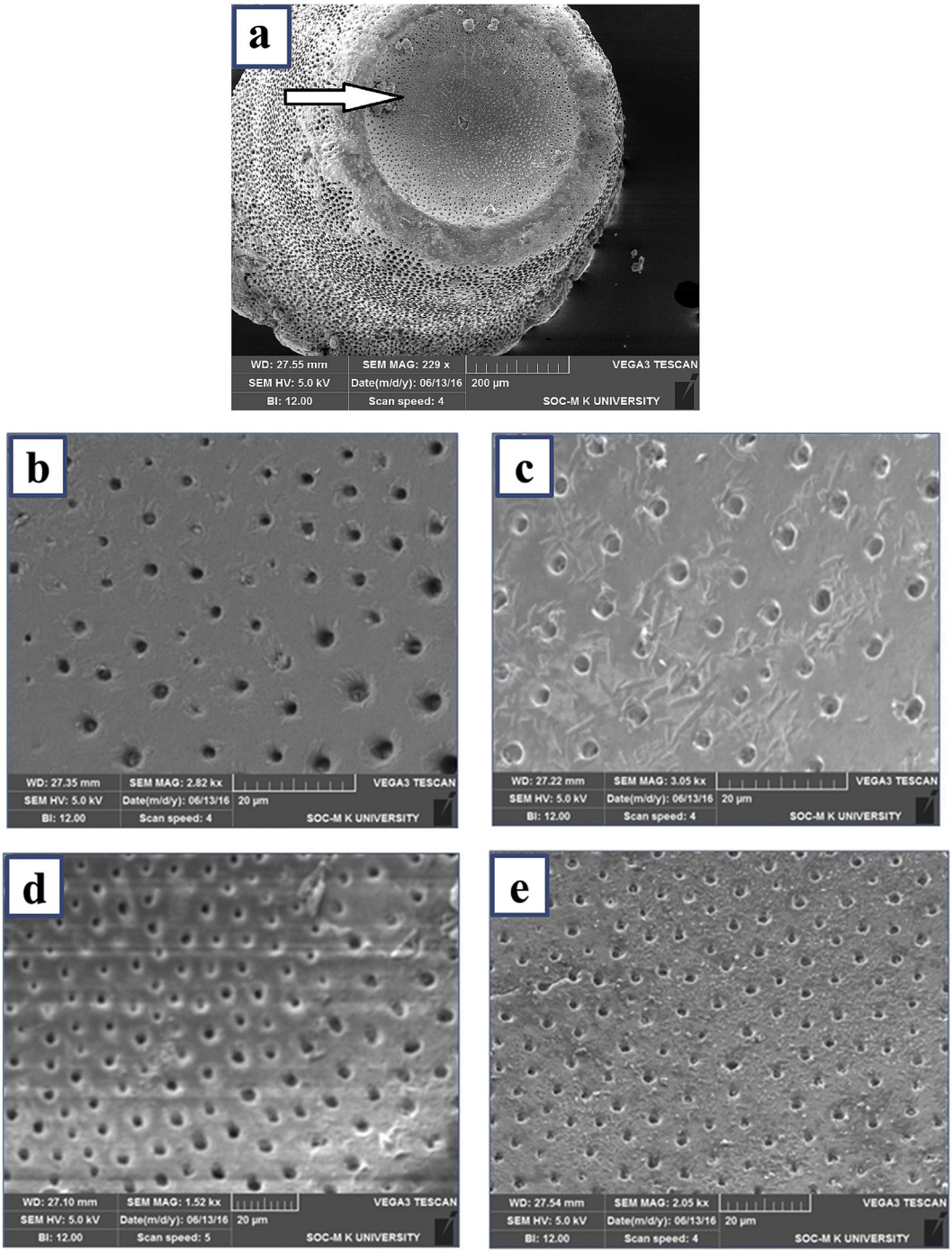

Figure 5. a) SEM image of basal surface of the spine of *S. virgulata* (arrow indicates the basal surface region) b) control (pH 8.2), c) pH 8.0, d) pH 7.8 and e) pH 7.6. The surface of spine looks weaker in low pH treated samples.

of acidic glycoprotein which is remarkably different from the exceptionally smooth cleavage surfaces of abiotic calcite.

FTIR vibrational bands of the present study confirmed the presence of $CaCO_3$ with sharp peak of in-plane carbonate bending (V_4) at 713 cm^{-1} and out-of-plane bending (V_2) between 875 cm^{-1} and 873 cm^{-1} for calcite in all the treatment pH and control. The previous studies revealed comparable V_4 splitting characteristic of the $CaCO_3$ and their spectrum compared to control of the present study was in good agreement (Balmain et al., 1999; Lee et al., 2011; Weir and Lipponcott, 1961; Kamba et al., 2013). Further vibrational bands of 3429–3414 cm^{-1} for V O–H (H_2O) and 1413–1411 cm^{-1} asymmetric stretching (V_3) of CO_3^{2-} trace the group change for calcite crystalline process (Lee et al., 2005; Gebauer et al., 2010). The low intense and broad absorption peak between 3425 and 3414 cm^{-1} (O–H stretching) ascribe the presence of structural water within calcite samples. Similar absorption peak 3637–3000 cm^{-1} was observed for crystallization of ACC (Cheng et al., 2019) and biogenic calcite spines 3400 cm^{-1} (Radha et al., 2010). Published reports prove that ACC act as precursor for calcite and aragonite skeletal structures of marine calcifiers (Addadi et al., 2003; Weiner et al., 2003; Weiss et al., 2002; Beniash et al., 1997; Politi et al., 2004, 2006, 2008; Aizenberg et al., 1996, 2002; Killian et al., 2009). Even though all the recognizable spectra for calcite crystalline process is similar in control and pH

Table 2. One-way ANOVA for the result of biomarker enzymes with different treated pH.

Biomarker Enzymes	Source of variation	SS	Df	MS	F	P
Acetylcholine Esterase	Between Groups	0.002598	3	0.000866	209.9697	$p < 0.001$
	Within Groups	1.65E-05	4	4.13E-06		
Catalase	Between Groups	0.000805	3	0.000268	306.8095	$p < 0.001$
	Within Groups	3.5E-06	4	8.75E-07		
Glutathione S-Transferase	Between Groups	0.000913	3	0.000304	243.4667	$p < 0.001$
	Within Groups	5E-06	4	1.25E-06		
Lipid Peroxidase	Between Groups	0.136762	3	0.045587	729.3973	$p < 0.001$
	Within Groups	0.00025	4	6.25E-05		
Reduced Glutathione	Between Groups	0.047788	3	0.015929	6707.14	$p < 0.001$
	Within Groups	9.5E-06	4	2.38E-06		

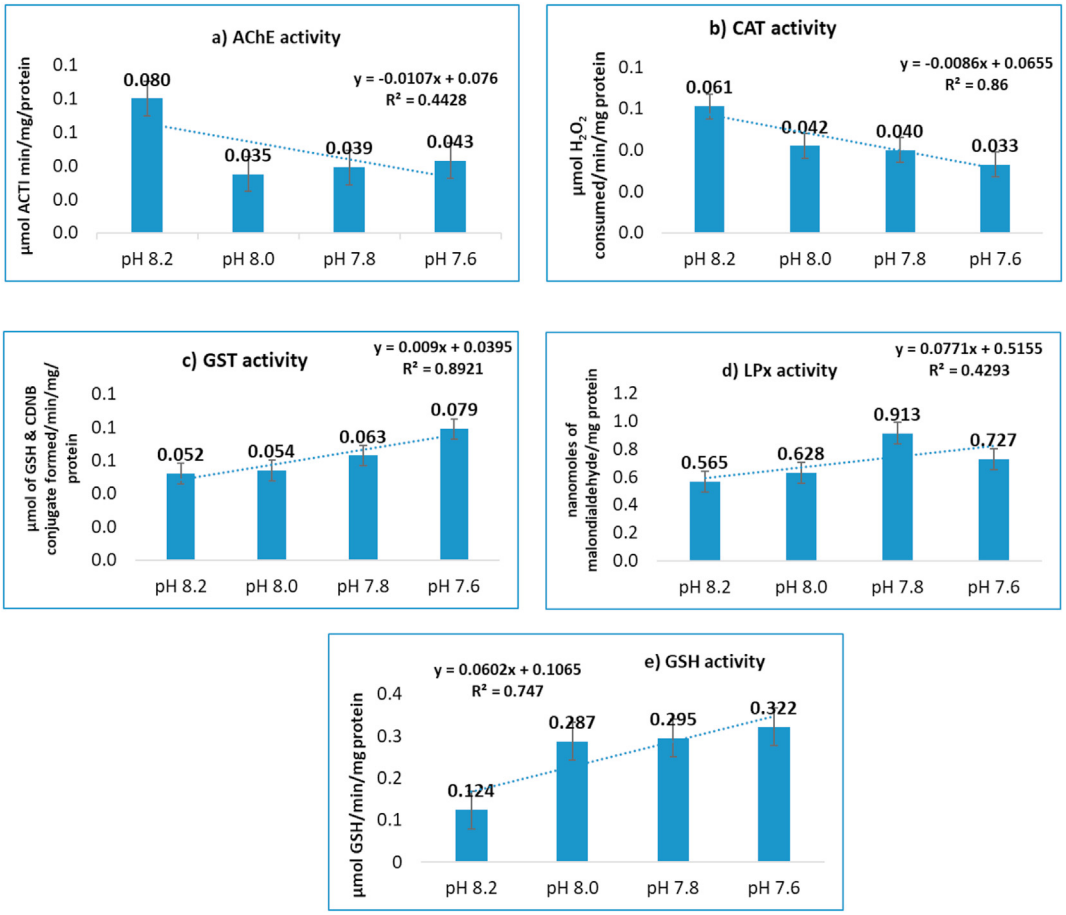

Figure 6. Physiological responses in gut tissues of *S. virgulata* at different pH exposure; a) AChE activity b) CAT activity c) GST activity d) LPx activity and e) GSH activity.

treatments; spectral band for O–H stretching in pH 8.0, 7.8 and 7.6 were typically broaden compared to control suggest a relative pH change influence on the crystal lattice of test shell.

Compared to pH 8.2 (control) and 8.0 (1413 cm^{-1}) the peak shift of C–O bond in 7.8 (1415 cm^{-1}) and 7.6 (1411 cm^{-1}) denote the disordered crystal lattice, similarly the shift in C–H bond vibration from 2928 cm^{-1} (control) to 2926 cm^{-1} (other pH treatments) confirm significant change in organic substances suggesting a variation in the crystal growth mechanism between animals exposed to high and low CO_2 conditions; in particular to ACC dehydration from ACC-H_2O to ACC and Calcite in a biologically controlled mechanism (Politi et al., 2008; Gong et al., 2012).

Similar to FTIR peak shift, the results of themogravimetric curve of the test samples too revealed significant weight loss impression between the test shell exposed to high (pH 8.2 and 8.0) and low CO_2 conditions (pH 7.8 and 7.6). Observable variation in FTIR spectral vibration for O–H structural water in four different pH exposures is well in agreement with the initial water loss with endothermic event at below 100 °C and further second and third weight loss for subsequent organic molecules in themogravimetric analysis. In TGA, the weight loss impression might be by phase transformation of $CaCO_3$form of calcite to unstable $CaCO_3$form (Lingaraju et al., 2002). Since both the control and treated samples remain unchanged when the temperature reached 750 °C, the result is considered as the total decomposition of calcium carbonate leaving alone the ash (Kamba et al., 2013; Mohamed et al., 2012). The rapid weight loss in this study reveals the endothermic behaviour of calcium carbonate. All of the thermogram values in present study showed four step weight loss

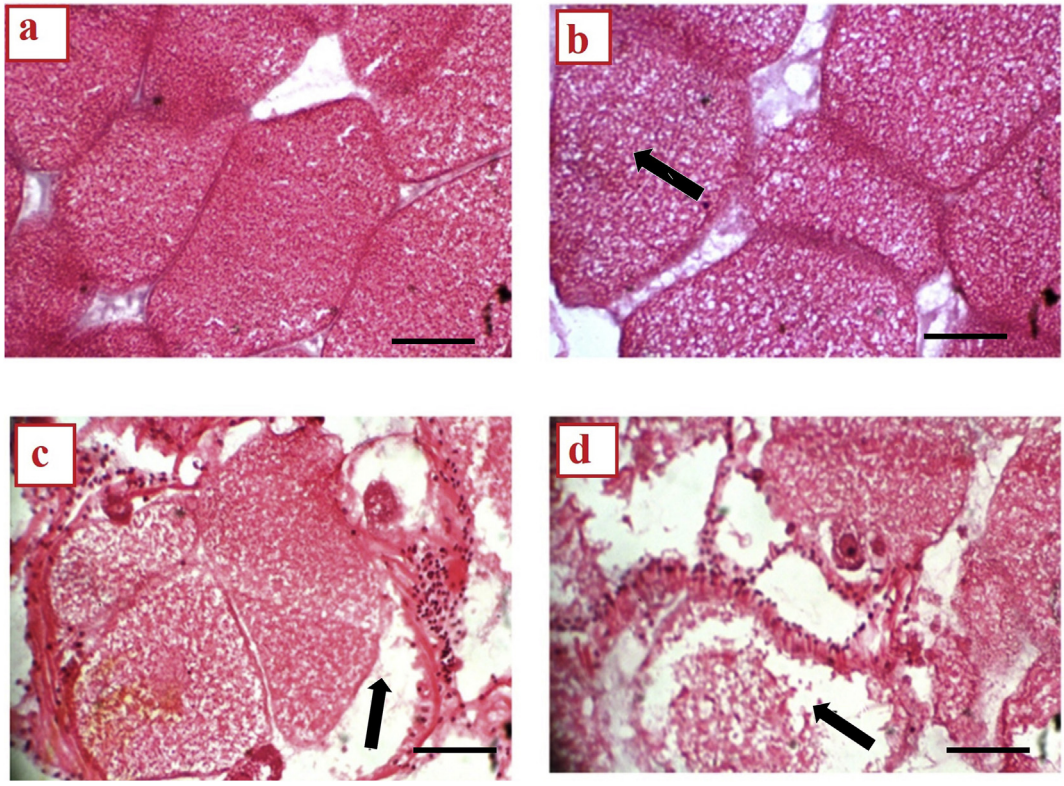

Figure 7. Light microscopic view of histology sections of *S. virgulata* gonads in 40X magnification shows ovaries exposed to a) control (pH 8.2) and different pH treatments b) pH 8.0 c) pH 7.8 and d) pH 7.6. The metachromasy of ovaries sections at the lumen of the gonad showed the cell disruption and rupture (arrow) visible in gonads exposed to pH 7.6 and pH 7.8. Gonad lesions were not found in ovary cells exposed to ambient pH but in near future acidification pH 8.0, the slight lesion found. All Scale bars indicate 50 μm.

nature, water loss (may be either loose or bound) from the membrane stage, bulk or micro calcium carbonate, the phase transformation of stable calcite to unstable $CaCO_3$ form after the water molecules from the carbonate lattice and complete volatilization. Eventually pH 7.6 shows a higher range of weight loss compare to the other pH levels (pH, 7.8, 8.0 and 8.2 (control), Ash was the final content of all samples. Such high sensitivity of weight loss may be connected to the weak O–H structural vibrations in the samples. Hence, TGA and FTIR results in this study enunciated the weakening of molecules in the dense $CaCO_3$ shell and their response to low pH (7.6 and 7.8) exposure.

XRD patterns of the present study reveal that the prevalence of calcite blooming in control samples compared to pH 7.6 and 7.8 (Wang et al., 2015). According to Goodwin (1969) and Amarowicz et al. (2012), sea urchin shells are mainly composed of calcium carbonate with the organic matrix. The 2θ value of 28.2° was not shown in pH 7.6 and 7.8 due to the characteristic changes in crystallinity of calcium carbonate shells. Calcium carbonate content had decreased in all low pH treatments, from pH 8.0 to 7.8 and 7.6. The combined results of FTIR, TGA and XRD revealed that a relative proportion of calcite in the shell was affected minimally to the near future CO_2 level scenario but mostly affected to high CO_2 level which substantially supports the theory that the reduced ocean pH and $CaCO_3$ availability will adversely affect the biomineralization process of sea urchin shell.

Morphology of sea urchin basal spine had clear and visible pores with corrosive surface. Similar results found on the portion of Aristotle's lantern of sea urchin which showed the large porous structure and irregularly shaped holes as a prevailing sign of corrosion and structural breaks due to increasing pCO_2 up to 1000 μatm and feeding rate of calcifying and non-calcifying algae (Asnaghi et al., 2013). Same kind of shell damages found in the degradation of calcium carbonate skeleton by less uniform size and increased inner matrix pores of ossicle pores in *A. lixula* under high magnification (Bray et al., 2014). Previous study of the dried shell mass of juvenile oyster was 39% lower in hypercapnic condition in comparison to normocapnic condition (Beniash et al., 2010). Low pH treatment made the negative attribution in size and stability of shell due to low calcium carbonate saturation in seawater (Watson et al., 2012). However, this analysis clearly indicated that the strength of calcium carbonate of *S. virgulata* lost its intensity in low pH (pH 7.6 and 7.8) treatments. The present study confirms the negative impact of ocean acidification on biomineralization process of sea urchins by affecting highly soluble crystal forming calcified tissues is in consistent with observed results of other marine calcifiers nevertheless the degree of impact varies from species to species (Dupont et al., 2010; Gazeau et al., 2013; Yao and Somero, 2014; Stillman and Paganini, 2015).

Results of all the five biomarkers were similar to the mussels integrated biomarker response demonstrated by Damiens et al. (2007) and were highly significant ($p < 0.01$) with one-way ANOVA. The present study denotes a moderate elicitation level of decreasing AChE for the near future level of CO_2 (pH 8) whereas a significant high elicitation level of decreasing AChE in pH 7.6 & 7.8. Acetylcholine esterase is a glycoprotein (Godoy-Reyes et al., 2019) found in variety of chemical structure but their functions in all species are similar (Hodges et al., 2018). AChE breaks down ester bond of acetylcholine and segregate into acetate and choline. AChE plays an important role in perception of prey and to sense deterioration condition in natural environment (Dos Santos Miron et al., 2005). Reduction of AChE indicates abnormal neurotransmission activity it could affect the whole nervous system. Several studies on choline esterase activity were important biomarker for assessing neurotoxicity impact on invertebrates and vertebrates (Jebali et al., 2011). Reduced AChE activity was recorded when the mussels transplanted from the unpolluted reference site to contaminated site (Damiens et al., 2007). AChE activity of the present study is similar to the findings of Priya et al.

(2016) on *Donax cuneatus* and Jiahuan et al. (2018) on *Acanthopagrus schlegelii* ensures the same negative effect of high CO_2 level exposures to marine organisms OA induced oxidative stress.

According to Lu et al. (2013) AChE and CAT had similar direction for decreasing activity when exposed to polybrominated diphenyl ethers. CAT is an antioxidant enzyme which have protective mechanism against H_2O_2 so that it is considered as one of the powerful biomarker tools. In the present study, the CAT activity showed decreasing sign in low pH exposures revealed the hydrogen peroxide stress. Similar result was recorded by Seguin et al. (2017) where CAT, GST & LPx revealed significant effects in transplanted mussels at contaminated sites. GST, LPx and GSH levels were increased in the present study. In particular, GST the member of the glutathione families that act against oxidative stress; showed increasing activity (Pereira et al., 2010). The main role of GST is considered as a fast recovery biomarker and the main role is to detoxify the cellular toxicity. GSH and LPx is said to be a precise signal for oxidative stress parameters and undergo slow recovery for bringing normal condition of the organism therefore it plays a significant role in pollutant assessment. LPx is assumed that they can propagate cytotoxic products and leads to DNA damage. Generally, the increased LPx enzyme is considered as the response of more contaminant. According to Herdege et al. (2011), pH induced changes intricate and affects conformational changes in chemoreceptor function and it leads to behavioural changes like olfactory function in invertebrates and vertebrates. Thus, biomarker enzymes in the present study showed negative physiological response to the animals exposed to low pH treatment compared to control. Since these assays are important in environmental health monitoring, possible impacts of hypercapnia induced physiological effect can be identified (Lam, 2009).

Gonad development is the process which comprises the continuous progression for each stage to become intact and sexually competent. In general, the impact on genital organs has more possible to deteriorate their reproduction and development (Havenhand et al., 2008). The gonads of sea urchin in different pH treatments of the present study revealed that pH 7.6 and 7.8 exposure had more impact on genital organs and particularly, ovarian cells become abruptly damaged when compare to control. Similar gonad lesions were found at Schafer and Kohler (2009) on female sea urchin after polycyclic aromatic hydrocarbon (PAH) where the results agree well in regard to gonad lesion in which, the high amount of degenerating previtellogenic oocytes exhibiting when the animal was treated with phenanthrene. Therefore, it seems the possible consequence that it will interrupt the successful fertilization in sea urchin, if even fertilized, the detrimental morphology of larval sea urchin (Moulin et al., 2011) in terms of reducing size and calcium carbonate skeletongenesis disruption (Kurihara, 2004, 2008).

Apart from the fertilization, lesions of sea urchin in many organs including gonads were characterized by Gilles and Pearse (1986), in which, close contact of diseased sea urchins with healthy individual led to infection. Consequently, the lesions progressed within 2 days for diseased urchin whereas in control sea urchin the tissue was regenerated in lesion area. Physiological response in the present study revealed a highly negative impact that could be the link between gonad lesion and fertilization deterioration. Bromhead et al. (2015) reported that the early stages of yellowfin tuna under extreme pCO_2 levels ($\geq$8800 μatm) showed significant reduction of larval survival.

The result of present study was in agreement to Frommel et al. (2016) report where the increasing damage in organs of yellowfin tuna showed decreased growth and endurance with high correlation. Gianguzza et al. (2014) documented that the temperature plays the significant role in fertilization success, in addition, the development rate of pH effect was dependent upon the temperature and eventually the development was slower at highest temperature. The results of FTIR TGA XRD and SEM imaging substantiate the negative impact of high CO_2 level exposures to sea urchin biomineralization process and the biomarker and histopathology findings bear strong evidence for the physiological stress experienced by *S. virgulata* was in accord to the findings on *T. gratilla* where the due impacts of low pH exposures alter the metabolism and energy demand of the animals in order to maintain the body acid-base balance (Stumpp et al., 2012; Collard et al., 2013; Dubois 2014).

5. Conclusion

The perspective of shell deformation, physiological response and gonad tissue damage in our study revealed ascertained manifestation when compared between control and treated animals. The IPCC predictions and on-going anthropogenic activity for CO_2 emissions are alarming for the year 2100. But the threats and effects of ocean acidification to marine flora and fauna are subtle which need to be studied in detail by micro and mesocosm experiments especially for marine calcifiers. The present study has proved that the reduced ocean pH negatively impacts the biochemical pathway of biomineralization process of shell formation by direct physiological stress on energy and ion supplies.

Declarations

Author contribution statement

M. Anand: Conceived and designed the experiments; Analyzed and interpreted the data.

K. Rangesh: Performed the experiments; Analyzed and interpreted the data; Wrote the paper.

M. Maruthupandy: Performed the experiments; Contributed reagents, materials, analysis tools or data.

G. Jayanthi and B. Rajeswari: Performed the experiments; Contributed reagents, materials, analysis tools or data.

R.J. Priya: Contributed reagents, materials, analysis tools or data.

Funding statement

This work was supported by University Grants Commission: India – New Zealand Educational Council (Sanction No: INZEC Project UGC F. No. 101-3/2014(IC), dt. 25.06.2014.

Data availability statement

Data included in article/supplementary material/referenced in article.

Declaration of interests statement

The authors declare no conflict of interest.

Additional information

No additional information is available for this paper.

Acknowledgements

The authors wish to thank the technicians of Central Instrumentation Center and DST purse scheme Madurai Kamaraj University for instrument facility. We very much thankful to our research collaborator Prof. Mary A. Sewell, The University of Auckland, New Zealand for manuscript proof reading, suggestions and improvement.

References

Addadi, L., Raz, S., Weiner, S., 2003. Taking advantage of disorder: amorphous calcium carbonate and its role in biomineralization. Adv. Mater. 15, 959–970.

Agaogullari, D., Kel, D., Gökçe, H., Duman, I., Öveçoğlu, M.L., Akarsubasi, A.T., Bilgiç, D., Oktar, F.N., 2012. Bioceramic production from sea urchins. Acta Phys. Pol., A 121 (1), 23–25.

Aizenberg, J., Ilan, M., Weiner, S., Addadi, L., 1996. Intracrystalline macromolecules are involved in the morphogenesis of calcitic sponge spicules. Connect. Tissue Res. 34, 255–261.

Aizenberg, J., Lambert, G., Weiner, S., Addadi, L., 2002. Factors involved in the formation of amorphous and crystalline calcium carbonate, a study of an ascidian skeleton. J. Am. Chem. Soc. 124, 32–39.

AmalaShajeeva, J., Neethiselvan, N., Sundaramoorthy, B., Masilan, K., Arunjenish, D., Rajakumar, M., Ravikumar, T., Baiju, V., 2017. Carbon Emission Due to Excess Fuel Consumption by the Trawlers of Thoothukudi, Southeast Coast of India. Carbon Management.

Amarowicz, R., Synowiecki, J., Shahidi, F., 2012. Chemical composition of shells from red (*Strongylocentrotusfranciscanu*) and green (*Strongylocentrotusdroeba-chiensis*) sea urchin. Food Chem. 133, 822–826.

Anandkumar, N., Thajuddin, 2013. Physico-chemical properties, seasonal variations in species composition and abundance of micro zooplankton in the Gulf of Mannar, India. Indian J. Geo-Marine Sci. 42 (3), 383–389.

APHA, 2005. Standard Methods for the Examination of Water and Wastewater, twenty-first ed. American Public Health Association/American water works association/ Water environment federation, Washington DC.

Arumugam, R., Kannan, R.R., Saravanan, K.J., Thangaradjou, T., Anantharaman, P., 2013. Hydrographic and sediment characteristics of seagrass meadows of the Gulf of Mannar marine biosphere reserve, South India. Environ. Monit. Assess.

Asnaghi, V., Chiantore, M., Mangialajo, L., Gazeau, F., Francour, P., 2013. Cascading effects of ocean acidification in a rocky subtidal community. PloS One 8 (4), e61978.

Balmain, J., Hannoyer, B., Lopez, E., 1999. Fourier transform infrared spectroscopy (FTIR) and X-ray diffraction analyses of mineral and organic matrix during heating of mother of pearl (Nacre) from the shell of the mollusc *Pinctada maxima*. J. Biomed. Mater. Res. 48, 749–754.

Beniash, E., Addadi, L., Weiner, S., 1999. Cellular control over spicule formation in sea urchin embryos: a structural approach. J. Struct. Biol. 125 (1), 50–62.

Beniash, E., Aizenberg, J., Addadi, L., Weiner, S., 1997. Amorphous calcium carbonate transforms into calcite during sea urchin larval spicule growth. P Roy Soc B-Biol Sci. 264, 461–465.

Beniash, E., Ivanina, A., Lieb, N.S., Kurochkin, I., Sokolova, M.I., 2010. Elevated level of carbon dioxide affects metabolism and shell formation in oysters *Crassostrea virginica*. Mar. Ecol. Prog. Ser. 419, 95–108.

Berman, A., Addadi, L., Kvick, A., Leiserowitz, L., Nelson, M., Weiner, S., 1990. Intercalation of sea urchin proteins in calcite: study of a crystalline composite material. Science 250, 664.

Berman, A., Addadi, L., Weiner, S., 1988. Interactions of sea-urchin skeleton macromolecules with growing calcite crystals - a study of intracrystalline proteins. Nature 331, 546–548.

Berman, A., Hanson, J., Leiserowitz, L., Koetzle, T.F., Weiner, S., Addadi, L., 1993. Biological control of crystal texture: a widespread strategy for adapting crystal properties to function. Science 259 (5096), 776–779.

Bray, L., Pancuci-Papadopulou, M.A., Hall-Spencer, J.M., 2014. Sea urchin response to rising pCO_2 shows ocean acidification may fundamentally alter the chemistry of marine skeletons. Mediterr. Mar. Sci. 15 (3), 510–519.

Brecevic, L., Nielsen, A.E., 1989. Solubility of amorphous calcium carbonate. J. Cryst. Growth 98 (3), 504–510.

Bromhead, D., Scholey, V., Nicol, S., Margulies, D., Wexler, J., Stein, M., Hoyle, S., Lennert-Cody, C., Williamson, J., Havenhand, J., Ilyina, T., Lehodey, P., 2015. The potential impact of ocean acidification upon eggs and larvae of yellowfin tuna (*Thunnusalbacares*). Deep-Sea Res. Pt. II 113, 268–279.

Brothers, C.J., McClintock, J.B., 2015. The effects of climate-induced elevated seawater temperature on the covering behavior, righting response, and Aristotle's lantern reflex of the sea urchin *Lytechinus variegatus*. J. Exp. Mar. Biol. Ecol. 467, 33–38.

Cheng, M., Sun, S., Peiyi, Wu., 2019. Microdynamic changes of moisture-induced crystallization of amorphous calcium carbonate revealed via in situ FTIR spectroscopy. Phys. Chem. Chem. Phys. 21, 21882–21889.

Clark, D., Lamare, M., Barker, M., 2009. Response of sea urchin pluteus larvae (Echinodermata: Echinoidea) to reduced seawater pH: a comparison among a tropical, temperate, and a polar species. Mar. Biol. 156, 1125–1137.

Clarkson, J.R., Price, T.J., Adams, C.J., 1992. Role of metastable phases in the spontaneous precipitation of calcium carbonate. J.Chem.Soc. Farada Trans. 88, 243–249.

Collard, M., Laitat, K., Moulin, L., Catarino, A.I., Grosjean, P., Dubois, P., 2013. Buffer capacity of the coelomic fluid in echinoderms. Comp. Biochem. Physiol. A, Mol. Integr. Physiol. 166, 199–206.

Coll-Lladó, C., Giebichenstein, J., Webb, P.B., Bridges, C.R., de la serrana, D.G., 2018. Ocean acidification promotes otolith growth and calcite deposition in gilthead sea bream (*Sparus aurata*) larvae. Nature Sci. Rep. 8, 8384.

Damiens, G., Gnassia-Barelli, M., Loques, F., Romeo, M., Salbert, V., 2007. Integrated biomarker response index as a useful tool for environmental assessment evaluated using transplanted mussels. Chemosphere 66, 574–583.

Decker, G.L., Morrill, J.B., Lennarz, W.J., 1987. Characterization of sea urchin primary mesenchyme cell sand spicules during biomineralization *in vitro*. Development 101, 297–312.

DosSantos Miron, D., Crestani, M., Rosa Shettinger, M., Maria Morsch, V., Baldisserotto, B., Angel Tierno, M., Moraes, G., Vieira, V.L., 2005. Effects of the herbicides clomazone, quinclorac and metsulfuron methyl on acetylcholinesterase activity in the silver catfish (*Rhamdiaquelen*) (Heptapteridae) Ecotoxicol. Environ. Saf. 61, 398–403.

Drozdova, A.L., Sharmankinaa, V.V., Zemnukhovab, L.A., Polyakovab, N.V., 2016. Chemical composition of spines and tests of sea urchins, 43 (6), 521–531.

Dubois, P., 2014. The skeleton of post metamorphic echinoderms in a changing world. Biol. Bull. 226, 223–236.

Dupont, S., Dorey, N., Thorndyke, M., 2010. What meta-analysis can tell us about vulnerability of marine biodiversity to ocean acidification? Estuar. Coast Shelf Sci. 89, 182–185.

Duquette, A., et al., 2017. Effects of ocean acidification on the shells of four Mediterranean gastropod species near a CO_2 seep. Mar. Pollut. Bull. 124 (2), 917–928.

Ellman, G.L., Gourtney, K.D., Andres, V., Featherstone, R.M., 1961. A new and rapid colorimetric determination of acetylcholinestarase activity. Biochem. Pharmacol. 7, 88–95.

Emerson, C.E., Reinardy, H.C., Bates, N.R., Bodnar, A.G., 2017. ocean acidification impacts spine integrity but not regenerative capacity of spines and tube feet in adult sea urchins, 4, 170140.

Frommel, A.Y., Margulies, D., Wexler, J.B., Stein, M.S., Scholey, V.P., Williamson, J.E., Bromhead, D., Nicol, S., Havenhand, J., 2016. Ocean acidification has lethal and sub-lethal effects on larval development of yellowfin tuna, *Thunnusalbacares*. J. Exp. Mar. Biol. Ecol. 482, 18–24.

Gattuso, J.P., Lavigne, H., 2009. Technical Note: approaches and software tools to investigate the impact of ocean acidification. Biogeosciences 6, 2121–2133.

Gazeau, F., Parker, L.M., Comeau, S., Gattuso, J.P., O'Connor, W.A., Martin, S., Pörtner, H.O., Ross, P.M., 2013. Impacts of ocean acidification on marine shelled molluscs. Mar. Biol. 160, 2207–2245.

Gebauer, D., Gunawidjaja, P.N., Ko, J.Y.P., Bacsik, Z., Aziz, B., Liu, L., Hu, Y., et al., 2010. Proto-calcite and proto-vaterite in amorphous calcium carbonates. Chem., Int. Ed. 49, 8889–8891.

Gianguzza, P., Visconti, G., Gianguzza, F., Sarà, G., Dupont, S., 2014. Temperature modulates the response of the thermophile sea urchin *Arbacialixula* early life stages to CO_2-driven acidification. Mar. Environ. Res. 93, 70–77.

Gilles, K., Pearse, J., 1986. Disease in sea urchins *Strongylocentrotuspurpuratus*: experimental infection and bacterial virulence. Dis. Aquat. Org. 1, 105–114.

Godoy-Reyes, T.M., Llopis-Lorente, A., García-Fernández, A., Gaviña, P., Costero, A.M., Martínez-Máñez, R., Sancenón, F., 2019. Acetylcholine-responsive Cargo Release Using Acetylcholinesterase-Capped Nanomaterials. Chemical Communications (RSC Publishing).

Gong, Y.U.T., Killian, C.E., Olson, I.C., Appathurai, N.P., Amasino, A.L., et al., 2012. Phase transitions in biogenic amorphous calcium carbonate. Proc. Natl. Acad. Sci. U.S.A. 109, 6088–6093.

Goodwin, T.W., 1969. Pigments of Echinodermata. In: Forkin, M., Scheer, B.T. (Eds.), Chemical Zoology, 3. Academic Press, New York, pp. 135–147.

Habig, W.H., Pabst, M.J., Jakoby, W.B., 1974. Glutothione S- transferases the first enzymatic step in mercapturic formation. J. Biol. Chem. 249, 7130–7139.

Hall-Spencer, J.M., Rodolfo-Metalpa, R., Martin, S., Ransome, E., Fine, M., Turner, S.M., Rowley, S.J., Tedesco, D., Buia, M.C., 2008. Volcanic carbon dioxide vents show ecosystem effects of ocean acidification. Nature 454, 96–99.

Hardege, J.D., Rotchell, J.M., Terschak, J., Greenway, G.M., 2011. Analytical challenges and the development of biomarkers to measure and to monitor the effects of ocean acidification. Trends Anal. Chem. 30 (8), 1320–1326.

Havenhand, J.N., Buttler, F.R., Thorndyke, M.C., Williamson, J.E., 2008. Near-future levels of ocean acidification reduce fertilization success in a sea urchin. Curr. Biol. 18, 651–652.

Hodges, G., Gutsell, S., Taylor, N.S., Brockmeier, E., 2018. Invertebrate model species in AOP development. In: Book: A Systems Biology Approach to Advancing Adverse Outcome Pathways for Risk Assessment, pp. 75–106.

Iglesias-Rodriguez, M.D., Anthony, K., Bijma, J., Dickson, A., Doney, S., Fabry, V.J., Feely, R.A., Gattuso, J.P., Lee, K., Riebsell, U., Saino, T., Turley, C., 2010. Towards an integrated global ocean acidification observation network Hall. In: J, Harrison, D.E. (Eds.), In Proceedings of OceanObs'09: Sustained Ocean Observations and Information for Society, 1. ESA, Venice, Italy, pp. 335–353, 21-25 September 2009.

Ilyina, T., Zeebe, R.E., Maier-Reimer, E., Heinze, C., 2009. Early detection of ocean acidification effects on marine calcification. Global Biogeochem. 23, 1–11.

IPCC, 2011. Workshop report of the intergovernmental panel on climate change workshop on impacts of ocean acidification on marine biology and ecosystems. In: Field, C.B., Barros, V., Stocker, D., Qin, K.J., Mach, G.K., Plattner, M.D., Tignor, M.M., Ebi, K.L. (Eds.), IPCC Working Group II Technical Support Unit. Carnegie Institution, Stanford, California, United States of America, p. 164.

Jebali, J., Ben-Khedher, S., Kamel, N., Ghedira, J., Bouraoui, Z., Boussetta, H., 2011. Characterization and evaluation of cholinesterase activity in the cockle *Cerastodermaglaucum*. Aquat. Biol. 13, 243–250.

Jiahuan, R., Wenhao, S., Xiaofan, G., Wei, S., Shanjie, Z., Maolong, H., Haifeng, W., Guangxu, L., 2018. Ocean Acidification impairs foraging behavior by interfering with olfactory neural signal transduction in black sea bream, *acanthopagrus schlegelii*. Front. Physiol. 9, 1592.

Kamba, A.S., Ismail, M., Ibrahim, T.A.T., Zakaria, Z.A.B., 2013. Synthesis and characterisation of calcium carbonate aragonite nanocrystals from cockle shell powder (*Anadaragranosa*). J. Nanomater. 2013, 1–9.

Kathiravan, K., Natesan, Usha, Vishnunath, R., 2017. Spatio-temporal variability of hydro-chemical characteristics of coastal waters of Gulf of Mannar marine biosphere reserve (GoMMBR), South India. Appl. Water Sci. 7, 361–373.

Kawahata, H., Fujita, K., Iguchi, A., et al., 2019. Perspective on the response of marine calcifiers to global warming and ocean acidification - behavior of corals and foraminifera in a high CO_2 world "hot house". Prog. Earth Planet Sci. 6, 5.

Killian, C.E., et al., 2009. Mechanism of calcite co-orientation in the sea urchin tooth. J. Am. Chem. Soc. 131, 18404–18409.

Kuffner, I.B., Andersson, A.J., Jokiel, P.L., Rodgers, K.S., Mackenzie, F.T., 2008. Decreased abundance of crustose coralline algae due to ocean acidification. Nat. Geosci. 1, 114–117.
Kurihara, H., 2008. Effects of CO_2-driven ocean acidification on the early developmental stages of invertebrates. Mar. Ecol. Prog. Ser. 373, 275–284.
Kurihara, H., Shirayama, Y., 2004. Effects of increased atmospheric CO_2 on sea urchin early development. Mar. Ecol. Prog. Ser. 274, 161–169.
Lam, P.K.S., 2009. Use of biomarkers in environmental monitoring. Ocean Coast Manag. 52, 348–354.
Lang, T., Wosniok, W., Baršienė, J., Katja-Broeg, K., Kopecka, J., Parkkonen, J., 2006. Liver histopathology in Baltic flounder (*Platichthysflesus*) as an indicator of biological effects of contaminants. Mar. Pollut. Bull. 488–496.
Lee, H.S., Ha, T.H., Mater, K.K., 2005. Fabrication of unusually stable amorphous calcium carbonate in an ethanol medium. Chem. Phys. 93, 376–382.
Lee, S.W., Jang, Y.N., Kim, J.C., 2011. Characteristics of the aragonitic layer in adult oyster shells, *Crassostreagigas*: structural study of myostracum including the adductor muscle scar. Evid. Based Complement Altern. Med. 742963-10.
Lingaraju, C., Narasimhulu, K.V., Gopal, N.O., Rao, J.L., Reddy, B.C.V., 2002. Electron paramagnetic resonance, optical and infrared spectral studies on the marine mussel *Arcaburnesis*hells. J. Mol. Struct. 608, 201–211.
Lu, G.H., Qi, P.D., Chen, W., 2013. Integrated biomarker responses of *Carassiusauratus* exposed to BDE-47, BDE-99 and their mixtures. Int. J. Environ. Res. 7 (3), 807–816.
Martin, S., Richier, S., Pedrotti, M.L., Dupont, S., Castejon, C., Gerakis, Y., Kerros, M.E., Oberhansli, F., Teyssie, J.L., Jeffree, R., Gattuso, J.P., 2011. Early development and molecular plasticity in the Mediterranean Sea urchin *Paracentrotus lividus* exposed to CO_2-driven acidification. J. Exp. Biol. 214, 1357–1368.
Michaelidis, B., Ouzounis, C., Paleras, A., Portner, H.O., 2005. Effects of long-term moderate hypercapnia on acid-base balance and growth rate in marine mussels *Mytilusgalloprovincialis*. Mar. Ecol. Prog. Ser. 293, 109–118.
Mohamed, M., Yusup, S., Maitra, S., 2012. Decomposition study of calcium carbonate in cockle shells. J. Eng. Sci. Technol. 7, 1–10.
Moron, M.S., Depierre, J.W., Mannervik, B., 1979. Levels of glutathione. Glutathione reductase and glutathione-S-transferase activity in rat lung and liver. Biochim. Biophys. Acta 582, 67–78.
Moulin, L., Catarino, A.I., Claessens, T., Duboisand, P., 2011. Effects of seawater acidification on early development of the intertidal sea urchin *Paracentrotuslividus* (Lamarck 1816). Mar. Pollut. Bull. 62, 48–54.
Neelakantan, K.S., 1998. Management Plan for Gulf of Mannar Marine Biosphere Reserve, Unpublished Report, Conservation of Forests, Wildlife Southern Region, Tirunelveli, p. 116.
Ohkawa, H., Ohishi, N., Yagi, K., 1979. Assay for lipid peroxides in animal tissues by thioharhituric acid reaction. Anal. Biochem. 95, 351–358.
Orr, J.C., Fabry, V.J., Aumont, O., Bopp, L., Doney, S.C., Feely, R.A., Gnanadesikan, A., Gruber, N., Ishida, A., Joos, F., Key, R.M., Lindsay, K., Maier-Reimer, E., Matear, R., Monfray, P., Mouchet, A., Najjar, R.G., Plattner, G.K., Rodgers, K.B., Sabine, C.L., Sarmiento, J.L., Schlitzer, R., Slater, R.D., Totterdell, I.J., Weirig, F., Yamanaka, Y., Yool, A., 2005. Anthropogenic ocean acidification over the twenty-first century and its impact on calcifying organisms. Nature 437, 681–686.
Pereira, C.D.S., Martın-Dıaz, M.L., Catharino, M.G.M., Cesar, A., Choueri, R.B., Taniguchi, S., Abessa, D.M., Bícego, M.C., Vasconcellos, M.B., Bainy, A.C., Sousa, E.C., Delvalls, T.A., 2010. Chronic contamination assessment integrating biomarkers' responses in transplanted mussels - a seasonal monitoring. Environ. Toxicol. 27 (5), 257–267.
Politi, Y., Arad, T., Klein, E., Weiner, S., Addadi, L., 2004. Sea urchin spine calcite forms via a transient amorphous calcium carbonate phase. Science (Washingto, DC, USA) 306, 1161–1164.
Politi, Y., et al., 2006. Structural characterization of the transient amorphous calcium carbonate precursor phase in sea urchin embryos. Adv. Funct. Mater. 16, 1289–1298.
Politi, Y., et al., 2008. Transformation mechanism of amorphous calcium carbonate into calcite in the sea urchin larval spicule. Proc. Natl. Acad. Sci. U.S.A. 105, 17362–17366.
Priya, R.J., Muthusamy, A., Maruthupandy, M., Beevi, A.H., 2016. Biomarker Response of ocean acidification induced hypercapnia on marine bivalve *Donaxcuneatus*, Linnaeus 1758. J. Aqua. Mar. Biol. 4 (2), 1–8.
Qu, C.F., Liu, F.M., Zheng, Z., Wang, Y.B., Li, X.G., Yuan, H.M., et al., 2017. Effects of ocean acidification on the physiological performance and carbon production of the Antarctic sea ice diatom *Nitzschia* sp. ICE-H. Mar. Pollut. Bull. 120 (1-2), 184–191.
Radha, A.V., Forbes, T.Z., Killian, C.E., P.U, P.A., Gilbert, Navrotsky, A., 2010. Transformation and crystallization energetics of synthetic and biogenic amorphous calcium carbonate. Proc. Natl. Acad. Sci. U. S. A. 107, 16438–16443.
Rajasegar, M., 2003. Physico-chemical characteristics of the Vellar estuary in relation to shrimp farming. Journal of environmental biology 24 (1), 95–101.
Riebsell, U., Fabry, V.J., Hansson, L., Gattuso, J.P., 2010. Guide to Best Practices for Ocean Acidification Research and Data Reporting, p. 263.
Ross, P.M., Parker, L., O'Connor, W.A., Bailey, E.A., 2011. The impact of ocean acidification on reproduction, early development and settlement of marine organisms. Water 3 (4), 1005–1030.
Schafer, S., Kohler, A., 2009. Gonadal lesions of female sea urchin (*Psammechinusmiliaris*) after exposure to the polycyclic aromatic hydrocarbon phenanthrene. Mar. Environ. Res.
Seguin, A., Mottier, A., Perron, C., Lebel, J.M., Serpentini, A., Costil, K., 2017. Sub-lethal effects of a glyphosate-based commercial formulation and adjuvants on juvenile oysters (*Crassostreagigas*) exposed for 35days. Mar. Pollut. Bull.
Sewell, M.A., Millar, R.B., Yu, P.C., Kapsenberg, L., Hofmann, G.E., 2014. Ocean acidification and fertilization in the Antarctic sea urchin *Sterechinus neumayeri*: the importance of polyspermy. Environ. Sci. Technol. 48, 713–722.
Sinha, A.K., 1972. Colorimetric assay of catalase. Anal. Biochem. 47 (2), 389–394.
Sivakumar, K., 2009. Seasonal variation in elemental composition of certain seaweeds from Mandapam and Kilakarai coast, Gulf of Mannar biosphere reserve. Acad. J. Plant Sci. 2 (2), 102–108.
Spicer, J.I., Raffo, A., Widdicombe, S., 2007. Influence of CO_2-related seawater acidification on extracellular acid–base balance in the velvet swimming crab *Necora puber*. Mar Biol. 151, 1117–1125.
Stillman, J.H., Paganini, A.W., 2015. Biochemical adaptation to ocean acidification. J. Exp. Biol. 218, 1946–1955.
Stumpp, M., Trubenbach, K., Brennecke, D., Hu, M.Y., Melzner, F., 2012. Resource allocation and extracellular acid-base status in the sea urchin *Strongylocentrotus droebachiensis* in response to CO_2 induced seawater acidification. Aquat. Toxicol. 110, 194–207.
Vidavsky, N., Addadi, S., Mahamid, J., Shimoni, E., Ben-Ezra, D., et al., 2014. Initial stages of calcium uptake and mineral deposition in sea urchin embryos. Proc. Natl. Acad. Sci. U.S.A. 111, 39–44.
Wang, Y.Y., Yao, Q.Z., Zhou, G.T., Fu, S.Q., 2015. Transformation of amorphous calcium carbonate into monohydrocalcite in aqueous solution: a biomimetic mineralization study. Eur. J. Mineral 27, 717–729.
Watson, S.A., Peck, L.S., Tyler, P.A., Southgate, P.C., Tan, K.S., Day, R.W., Morley, S.A., 2012. Marine invertebrate skeleton size varies with latitude, temperature and carbonate saturation: implications for global change and Ocean Acidification. Global Change Biol. 18, 3026–3038.
Weiner, S., Levi-Kalisman, Y., Raz, S., Addadi, L., 2003. Biologically formed amorphous calcium carbonate. Connect. Tissue Res. 44 (Suppl.1), 214–218.
Weir, C.E., Lippincott, E.R., 1961. Infrared studies of aragonite, calcite, and vaterite type structures in the borates, carbonates, and nitrates. J. Res. Natl. Bur. Stand. 65 (3), 173–183.
Weiss, I.M., Tuross, N., Addadi, L., Weiner, S., 2002. Mollusk larval shell formation, amorphous calcium carbonate is a precursor phase for aragonite. J. Exp. Zool. 293, 478–491.
Wolf-Gladrow, D.A., Zeebe, R.E., Klaas, C., Kortzinger, A., Dickson, A.G., 2007. Total alkalinity: the explicit conservative expression and its application to biogeochemical processes. Mar. Chem. 106, 287–300.
Wolpert, L., Gustafson, T., 1961. Studies on the cellular basis of morphogenesis of the sea urchin embryo. Development of the skeletal pattern. Exp. Cell Res. 25, 311–325.
Yang, Y., Hansson, L., Gattuso, J.P., 2016. Data compilation on the biological response to ocean acidification: an update. Earth Syst. Sci. Data 8, 79–87.
Yao, C.L., Somero, G.N., 2014. The impact of ocean warming on marine organisms. Chin. Sci. Bull. 59, 468–479.
Zeebe, R.E., 2012. History of seawater carbonate chemistry, atmospheric CO2, and ocean acidification. Annu. Rev. Earth Planet Sci. 40 (1), 141–165.